

# GO BEYOND EARTH: UNDERSTANDING HUMAN ACTIONS AND SCENES IN MICROGRAVITY ENVIRONMENTS

Di Wen<sup>1\*</sup> Lei Qi<sup>1\*</sup> Kunyu Peng<sup>1†</sup> Kailun Yang<sup>2</sup> Fei Teng<sup>2</sup> Ao Luo<sup>3</sup> Jia Fu<sup>4,5</sup>

Yufan Chen<sup>1</sup> Ruiying Liu<sup>1</sup> Yitian Shi<sup>1</sup> M. Saquib Sarfraz<sup>1,6</sup> Rainer Stiefelhagen<sup>1</sup>

<sup>1</sup>Karlsruhe Institute of Technology <sup>2</sup>Hunan University <sup>3</sup>Waseda University

<sup>4</sup>KTH Royal Institute of Technology <sup>5</sup>RISE Research Institutes of Sweden

<sup>6</sup>Mercedes-Benz Tech Innovation

## ABSTRACT

Despite substantial progress in video understanding, most existing datasets are limited to Earth’s gravitational conditions. However, microgravity alters human motion, interactions, and visual semantics, revealing a critical gap for real-world vision systems. This presents a challenge for domain-robust video understanding in safety-critical space applications. To address this, we introduce MicroG-4M, the first benchmark for spatio-temporal and semantic understanding of human activities in microgravity. Constructed from real-world space missions and cinematic simulations, the dataset includes 4,759 clips covering 50 actions, 1,238 context-rich captions, and over 7,000 question–answer pairs on astronaut activities and scene understanding. MicroG-4M aims to support three core tasks: fine-grained multi-label action recognition, temporal video captioning, and visual question answering, thereby enabling a comprehensive evaluation of both spatial localization and semantic reasoning in microgravity contexts. We establish baselines using state-of-the-art models. All data, annotations, and code are available at <https://github.com/LEI-QI-233/HAR-in-Space>.

## 1 INTRODUCTION

Yuri Gagarin’s historic flight in 1961 marked the beginning of human space exploration. Since then, significant milestones have been achieved, including crewed lunar landings, the continuous operation of the International Space Station (ISS) for over 25 years, and the participation of more than 650 individuals in space missions Moskowitz & Wolf (2025). With numerous planned crewed missions in the near future, the frequency and complexity of human activities in space are expected to increase substantially. In this context, ensuring the safety, enhancing the operational efficiency of space missions, and safeguarding the health and well-being of astronauts are of paramount importance.

With the rapid advancement of artificial intelligence, the integration of robotic systems aboard spacecraft is anticipated in the near future. These systems will assist astronauts in routine and mission-critical tasks. Consequently, there is a growing demand for the development of deep learning-based scene understanding and action recognition methods tailored specifically for the unique challenges posed by the microgravity environment.

Human action recognition Wang et al. (2023a); Feichtenhofer (2020); Feichtenhofer et al. (2019), scenario captioning Chen et al. (2024), and Visual Question Answering (VQA) Hu et al. (2023) are essential for intelligent human-robot collaboration, particularly in space, where precise perception and understanding of astronauts’ actions and their surrounding context are crucial for ensuring operational safety, efficiency, and autonomous assistance under constrained conditions. This capability is crucial for ensuring mission efficiency, enhancing astronaut safety, and providing autonomous assistance in the confined and complex conditions of space habitats. Numerous human action recognition datasets

---

\*Equal contribution.

†Corresponding author: kunyu.peng@kit.edu

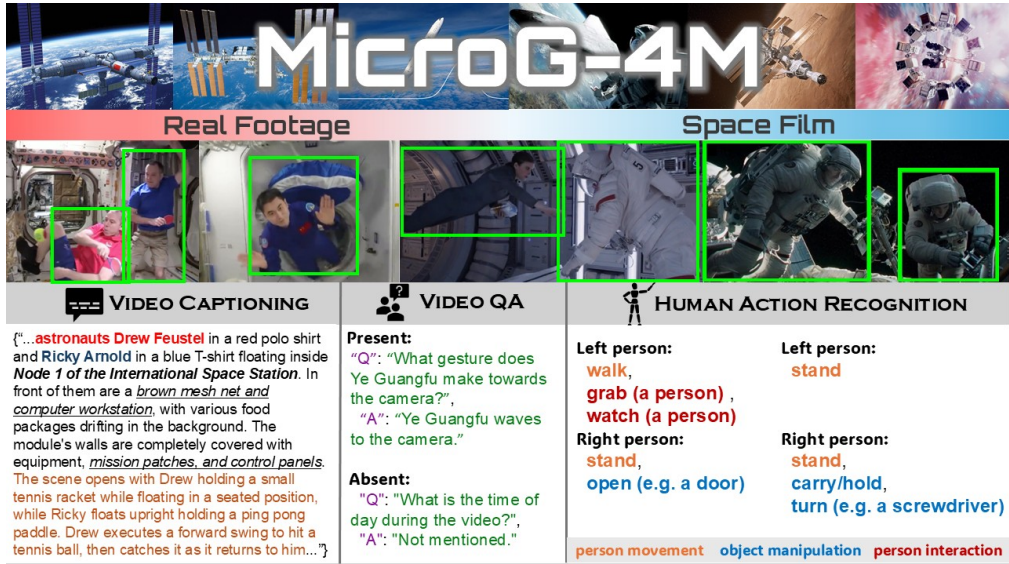


Figure 1: An illustration of the MicroG-4M, containing videos from real and simulated microgravity environments (e.g., movies). The dataset supports benchmarks for three tasks: (1) video captioning, (2) video question answering, and (3) fine-grained human action recognition under microgravity.

and video caption datasets have been developed, playing an important role in various research areas within computer vision and in industrial applications Camarena et al. (2023); Pareek & Thakkar (2021); Al-Faris et al. (2020); Le et al. (2022).

However, most of the existing datasets for video scenario captioning and action recognition are recorded on Earth without microgravity settings, e.g., Kinetics400 Kay et al. (2017), AVA Gu et al. (2018), FineGym Shao et al. (2020), and ActivityNet Captions Chen et al. (2019).

Human actions in space depart markedly from their terrestrial counterparts because microgravity removes gravity-aligned orientation and reliable support surfaces. Basic behaviors—standing, locomotion, eating, and manual manipulation—follow different kinematics and contact patterns Hagio et al. (2022). Standing becomes orientation-invariant, often maintained via foot restraints or hand-holds rather than ground support; locomotion is achieved by drifting or pulling along structures rather than gait; and manipulation frequently involves releasing or catching free-floating objects instead of placing or picking from a surface. These shifts violate terrestrial orientation, support/contact, and object-dynamics priors, which helps explain the degradation of Earth-trained Human Action Recognition (HAR) models in orbit and motivates a microgravity-specific benchmark.

To address this gap, we introduce *MicroG-4M*, a new video benchmark specifically designed for spatio-temporal and semantic understanding of human activities in microgravity. The name “4M” reflects four characteristics: *Multi-source* (Real mission footage and physically plausible film), *Multimodal* (RGB + text annotations), *Multi-task* (HAR, captioning, VQA), and *Microgravity*.

MicroG-4M comprises 4,759 three-second video clips drawn from public YouTube footage of real space missions and carefully selected, realistic space-themed films to augment scenario diversity and coverage. The clips span scenes inside the ISS, the Tiangong Space Station, crewed spacecraft cabins, and extravehicular activities. The corpus contains more than 390,000 annotated frames with bounding boxes for each visible individual and 13,000+ action labels covering 50 distinct actions. In addition, it includes 1,238 descriptive clip captions created by human annotators and 7,000+ open-ended question–answer pairs aimed at assessing factual, causal, and counterfactual understanding of scenes in microgravity. Both captions and QA annotations were carefully curated through multiple refinement rounds and data selection stages, ensuring high semantic fidelity, contextual accuracy, and relevance to the microgravity setting. Together, these resources enable multi-label spatio-temporal detection, fine-grained action recognition, caption generation, and VQA within a single dataset. To evaluate existing methods, we build the first comprehensive benchmark for these tasks, dubbed **MicroG-Bench**. We evaluate representative video encoders (SlowFast Feichtenhofer et al. (2019), X3D Feichtenhofer (2020), and MViT Li et al. (2022)) for human action recognition and leading vision-language models (e.g., InternVideo Wang et al. (2022), Gemini 1.5 Pro Anil et al. (2023),

GPT-4o [Hurst et al. \(2024\)](#)) for captioning and VQA tasks. Across all evaluated subtasks, state-of-the-art terrestrial models experience significant performance degradation, underscoring the unique challenges posed by microgravity environments, such as arbitrary orientations, floating objects, and confined spacecraft interiors. These results highlight the necessity of dedicated benchmarks to facilitate the advancement of more robust and generalizable AI systems tailored for space applications. MicroG-Bench, therefore, provides a unified, fair yardstick that will guide the development of more robust and generalizable perception and language systems for astronaut assistance and autonomous mission operations. We summarize our contributions as follows. We present MicroG-4M, the first video-based dataset for activity recognition and scene understanding specifically designed for the microgravity environment. Additionally, we establish the first benchmark to evaluate state-of-the-art human action recognition methods and vision-language models for fine-grained action recognition and video captioning/QA in this unique setting.

## 2 RELATED WORK

**Vision-Based Understanding in Microgravity and Space Environments.** Microgravity challenges terrestrial vision assumptions, requiring perception models for space habitats. Early work showed traditional SLAM to be unreliable, leading to robust alternatives with visual-inertial fusion, semantic mapping, CAD-informed constraints [Soussan et al. \(2022\)](#); [Mao et al. \(2024\)](#); [Miller et al. \(2022\)](#); [Tweddle et al. \(2015\)](#), and validated on platforms like Astrobee [Kang et al. \(2024\)](#). Real-time vision has also enabled dynamic tasks such as target tracking and scene change detection [Oestreich et al. \(2021\)](#); [Dinkel et al. \(2024\)](#). Research has shifted toward interaction, including astronaut pose recovery [Gan et al. \(2023\)](#); [Ouyang et al. \(2025\)](#), gesture recognition [Lingyun et al. \(2020\)](#); [Gao et al. \(2020\)](#), and EMG-based input [Assad et al. \(2013\)](#). Yet, high-level semantic understanding of astronaut actions and intent remains limited. Current assistants like CIMON [Eisenberg et al. \(2024\)](#) provide basic perception but lack contextual reasoning. To address this, we propose a unified benchmark for action recognition, video captioning, and visual question answering in space operations.

**Datasets for Action Detection, Video Captioning, and VQA.** Progress in video understanding has been largely enabled by the introduction of benchmark datasets across action detection, captioning, and VQA. For action detection, early datasets such as UCF101 [Soomro et al. \(2012\)](#) and HMDB51 [Kuehne et al. \(2011\)](#) provided trimmed classification tasks, later extended by Kinetics [Kay et al. \(2017\)](#) and ActivityNet [Caba Heilbron et al. \(2015\)](#) to large-scale, untrimmed settings with diverse action categories. AVA [Gu et al. \(2018\)](#) further introduced spatio-temporal annotations for atomic actions, enabling fine-grained multi-label detection in realistic scenes. Video captioning evolved from MSVD [Chen & Dolan \(2011\)](#) and MSR-VTT [Xu et al. \(2016\)](#), which paired short clips with multiple sentences, to dense captioning in untrimmed videos via ActivityNet Captions [Krishna et al. \(2017\)](#) and procedural datasets like YouCook2 [Zhou et al. \(2018\)](#). Multilingual benchmarks such as VATEX [Wang et al. \(2019\)](#) expanded the task to cross-lingual settings with high-quality parallel annotations. In VQA, static image datasets like VQA v2.0 [Goyal et al. \(2017\)](#) and CLEVR [Johnson et al. \(2017\)](#) laid the foundation for compositional reasoning, while TGIF-QA [Jang et al. \(2017\)](#), MovieQA [Tapaswi et al. \(2016\)](#), and TVQA [Lei et al. \(2018\)](#) introduced temporal and multimodal reasoning in video. Recent efforts such as NExT-QA [Xiao et al. \(2021\)](#) and CLEVRER [Yi et al. \(2020\)](#) focus on causal inference and counterfactual reasoning. However, existing datasets are constrained to terrestrial environments and lack domain-specific complexities inherent to space-based activities. To bridge this gap, we introduce the first benchmark for video captioning and VQA in microgravity, enabling the evaluation of vision-language models in long-horizon, space-relevant scenarios.

**Fine-Grained Human Action Recognition.** Fine-grained video-based action recognition [Gritsenko et al. \(2023\)](#); [Chung et al. \(2021\)](#) aims to detect fine-grained, indivisible human actions in both single- and multi-person videos. Unlike standard clip-level recognition, atomic action localization requires frame-level, multi-label classification with spatio-temporal bounding box predictions. To tackle this, CNN-based [Wang et al. \(2023a\)](#); [Feichtenhofer \(2020\)](#); [Feichtenhofer et al. \(2019\)](#) and transformer-based [Ryali et al. \(2023\)](#); [Wang et al. \(2023a\)](#); [Li et al. \(2022\)](#); [Wang et al. \(2023b\)](#); [Peng et al. \(2022\)](#); [Gritsenko et al. \(2023\)](#) models have been adapted by adding multi-label heads, bounding box regressors, and region-of-interest modules. Notably, [Ryali et al. \(2023\)](#) introduced a hierarchical vision transformer balancing accuracy and efficiency, while [Wang et al. \(2023a\)](#) proposed a dual-masked autoencoder for improved video pretraining. In this work, we evaluate such HAR methods for the first time in microgravity scenarios.

### 3 COLLECTION METHODOLOGY

We aim to construct a dataset comprising authentic footage recorded aboard the International Space Station and other spacecraft, as well as films that realistically depict microgravity conditions. In the following, we introduce our comprehensive pipeline for collecting, assembling, filtering, and annotating the MicroG-4M dataset, which supports multi-label spatio-temporal action detection, video captioning, and video question answering tasks from Internet-sourced videos.

**Raw Video Information Collection.** Video sources primarily include genuine microgravity footage from actual spacecraft missions and selected cinematic clips known for their realistic depictions of weightlessness. Authentic spacecraft videos were mainly retrieved from online video platforms, while cinematic clips were manually chosen based on their fidelity to real microgravity conditions. All videos were standardized to a resolution of  $480p$  to maintain consistency. The final dataset comprises approximately 5,000 three-second clips, predominantly composed of authentic spacecraft footage.

**Dataset Assembly Pipeline.** We established an automated pipeline to preprocess and structure raw videos, enabling consistent and accurate downstream annotation. The pipeline consists of three main stages: video segmentation, filtering, and automated bounding-box annotation.

Raw Video Trimming. Raw videos are trimmed into uniform three-second clips at 30 fps, discarding shorter segments to maintain temporal consistency.

Filtering. Video clips undergo automatic filtering based on person detection and scene-transition analysis. Specifically, we employed YOLOv11 [Khanam & Hussain \(2024\)](#) for human detection and PySceneDetect [Castellano](#) to identify abrupt scene changes, discarding clips with insufficient human-action content or disrupted temporal continuity.

Bounding-box Annotation. Person bounding boxes are automatically annotated using YOLOv11 [Khanam & Hussain \(2024\)](#) detection combined with BoT-SORT tracking [Aharon et al. \(2022\)](#). To enhance annotation accuracy, adaptive strategies were employed by assessing video motion intensity using sparse optical flow methods [Jeannin & Divakaran \(2001\)](#); [Ali \(2013\)](#); [Szeliski \(2010\)](#). Annotation parameters were dynamically adjusted accordingly to optimize computational efficiency and annotation precision. The resulting structured annotations include bounding-box coordinates, unique identities, and detection confidence scores.

**Manual Video Screening.** Following automated preprocessing, an additional manual verification step was performed to ensure dataset purity and environmental consistency. Specifically, each generated video clip was individually reviewed to exclude terrestrial scenes, such as ground-based footage or pre-launch preparations, thereby retaining only those segments clearly depicting human activities under authentic microgravity conditions. This rigorous screening process ensured semantic precision and enhanced the overall reliability of the dataset.

**Action Label Annotation.** In this phase, we derive a microgravity-tailored action taxonomy from AVA’s 80 atomic actions [Gu et al. \(2018\)](#). To ensure environmental applicability and semantic continuity, we (i) exclude actions that are physically inapplicable in space (e.g., water- or ground-specific), (ii) merge near-duplicates into unified categories, and (iii) introduce context-aware semantic adjustments. To disambiguate visually or semantically similar actions, we define explicit differentiation criteria that standardize annotation decisions. Each three-second clip is treated as a self-contained unit: for every detected individual, annotators assign up to five visible or inferable action labels per clip. The verified annotations are exported as structured CSV files for downstream training and evaluation. Retaining AVA class names while re-grounding their semantics in microgravity enables fair Earth→space comparisons without altering the label space.

**Caption and VQA Annotation.** For caption annotation, we developed a rigorous protocol that combines detailed visual analysis of video content with supplementary contextual information sourced from official aerospace agency documentation to ensure both accuracy and authority. Specifically, we compiled and referenced mission objectives, crew rosters, and official reports from various space agencies across different countries and missions, enabling precise identification of individual astronauts. Furthermore, we utilized historical spacecraft layout diagrams and functional distribution maps of the spacecraft cabins to accurately determine the astronaut’s location within the spacecraft as well as the equipment inside it. In parallel, annotators conducted thorough reviews of the complete video sequences, identifying subtle differences between adjacent frames to precisely



Figure 2: An illustration of the statistics of the dataset and the annotation samples. Word clouds of the (a) Caption, (b) Question, and (c) Answer from our MicroG-4M dataset are provided. The label statistics of the fine-grained human action recognition are provided in (d), which showcases the annotation number per action group (*i.e.*, Object Manipulation (OM), Person Interaction (PI), Person Movement (PM)). The distribution of person counts per video clip is visualized in (e). On the bottom right, one annotation sample from MicroG-4M is provided.

describe astronauts’ actions, physical appearances, and interactions with the environment. These high-quality captions provide strong semantic grounding to support downstream tasks such as action recognition and context-aware retrieval.

For Video Question Answering (VQA), we adopted a structured approach based on Heilman & Smith (2009), formulating diverse questions using standard interrogative forms. Based on the complexity of the video captions, Large Language Models (LLMs) generate a proportional number of candidate question-answer pairs, explicitly filtering out cases with missing or uncertain information. These candidates are then ranked by the LLMs according to logical consistency, linguistic fluency, semantic relevance, and informational value. Subsequently, multiple rounds of human-assisted review and prompt adjustment are employed to eliminate any hallucinated or fabricated content produced by the LLMs. Finally, a concise set of six diverse and content-rich QA pairs is selected for each video, ensuring comprehensive coverage from broad contextual understanding to detailed actions.

**Annotation Quality Control.** During the annotation phase, a team of 9 annotators collaboratively worked on labeling the fine-grained human actions, generating video captions, and crafting VQA pairs. To ensure high annotation quality, a comprehensive cross-verification protocol was implemented throughout the process, supported by group discussions to resolve disagreements and reach consensus. For the captioning and VQA tasks, all entries were further subjected to a semantic consistency check utilizing LLMs, followed by iterative human review to enhance both linguistic clarity and factual accuracy. This layered validation pipeline, combining automated and manual strategies, ensured the reliability and coherence of the annotations across all modalities. As a result, we introduce the MicroG-4M dataset, an extensively curated benchmark explicitly designed for fine-grained, multi-label, spatiotemporal action recognition, captioning, and VQA under microgravity conditions. This dataset sets a new foundation for advancing robust scene understanding and human activity analysis in space-based environments.

## 4 DATASET COMPOSITION

We release the *MicroG-4M* dataset, comprising the following subsets:

**Fine-Grained Human Action Recognition Subset:** Contains fine-grained, multi-label annotations for spatiotemporal human action detection, comprising 4,759 manually annotated three-second video clips from authentic microgravity environments. Each clip includes annotations for up to five distinct actions per detected individual. The 50 action labels are organized into three categories: Object Manipulation (4,976 annotations, 37.60%), Person Interaction (4,288 annotations, 32.34%), and Person Movement (3,987 annotations, 30.07%). Figure 2(d) illustrates the distribution of these

categories in both real and simulated video clips, while Figure 2(e) shows the distribution of person counts per clip, highlighting the diversity of social configurations. Overall, the subset contains 13,261 action annotations, including 9,610 from real footage, 3,651 from simulated sources, and 390,000 bounding box annotations.

**Video Caption Subset:** Comprises 1,238 detailed, semantically rich descriptions validated against official aerospace agency documentation for astronaut identities, spacecraft locations, actions, appearances, and interactions. Each caption corresponds uniquely to one video clip. The word cloud visualization in Figure 2(a) provides insights into frequently mentioned terms and concepts, illustrating the thematic and semantic distribution of the captions.

**Visual Question Answering (VQA) Subset:** Includes 7,428 structured QA pairs, systematically generated and refined via LLMs to ensure linguistic fluency, semantic relevance, and comprehensive coverage of detailed actions and broader context, with each of the 1,238 video clips associated with up to six diverse QA pairs. Figure 2(b) and (c) show word clouds for questions and answers separately, revealing prevalent inquiry types and common semantic patterns within the dataset.

Figure 2 presents representative video clips from the dataset, demonstrating typical annotation examples and highlighting the visual and semantic diversity of the dataset. More details regarding the dataset can be found in the appendix.

## 5 EXPERIMENTS VALIDATING

### 5.1 BENCHMARK PROTOCOL

**Data Split.** We partition the dataset into training, validation, and test subsets in a 7:1:2 ratio. Row-level distribution is as follows: Training set: 9,266 records (69.93% of 13,251); Validation set: 1,329 records (10.03% of 13,251); Test set: 2,656 records (20.04% of 13,251). Video-level distribution is as follows: Training set: 3,331 videos (69.99% of 4,759); Validation set: 475 videos (9.98% of 4,759); Test set: 953 videos (20.03% of 4,759).

**Baselines for Fine-Grained HAR in Microgravity Scenarios.** For fine-grained action recognition, we evaluate well-established baselines from video-based human action recognition, including transformer-based models (MViTv1 [Fan et al. \(2021\)](#), MViTv2 [Li et al. \(2022\)](#)) and CNN-based models (I3D [Carreira & Zisserman \(2017\)](#), SlowFast [Feichtenhofer et al. \(2019\)](#), X3D [Feichtenhofer \(2020\)](#), C2D [Feichtenhofer et al. \(2019\)](#)). These widely used architectures cover both paradigms and allow us to assess generalization to the unique spatiotemporal dynamics of microgravity. All models are initialized with Kinetics400 [Kay et al. \(2017\)](#) pretrained weights for better convergence.

**Baseline methods for Video Captioning and QA in Microgravity Scenarios.** For video captioning and question answering in microgravity, we evaluate strong baselines, including open-source models (VideoChatGPT [Li et al. \(2023\)](#), mPLUG-Owl-3 [Ye et al. \(2025\)](#), LLaVA-Next [Li et al. \(2024\)](#), VideoLLaVa [Lin et al. \(2024\)](#), Qwen-2.5-VL [Bai et al. \(2025\)](#), InternVideo [Wang et al. \(2022\)](#)) and closed-source models (GPT-4o [Hurst et al. \(2024\)](#), Gemini 1.5 Pro [Reid et al. \(2024\)](#)). Open-source models offer reproducibility via public weights and code, while closed-source models serve as upper-bound references. This mix enables both transparent analysis and comprehensive evaluation of video-language understanding in microgravity.

**Cross-domain transfer protocol.** To quantify the microgravity-induced domain gap, we use a fixed transfer setup: models pretrained on Kinetics are fine-tuned on AVA [Gu et al. \(2018\)](#) with matched settings, then evaluated zero-shot on MicroG-4M. For terrestrial contrast, we test on JHMDB (Split 1) [Jhuang et al. \(2013\)](#) with the overlapping action set and standard protocol. This isolates domain effects (microgravity vs. Earth) from implementation choices; evaluation details in Sec. 5.

**Evaluation Metrics for Fine-Grained HAR.** Our evaluation metrics include mAP@0.5, F1 score, recall, and AUROC, all calculated using the macro method. Among these, mAP@0.5 is the primary metric for measuring average detection accuracy per category and thus comprehensively evaluating the model’s action recognition performance in a microgravity environment. Per-class threshold sweeps are provided in the appendix.

**Evaluation Metrics for Video Caption and QA.** We adopt standard automatic evaluation metrics, including CIDEr [Vedantam et al. \(2015\)](#), BLEU-4 [Papineni et al. \(2002\)](#), ROUGE-L [Lin \(2004\)](#),

Table 1: Performance of models fine-tuned on MicroG-4M, evaluated on the validation and test sets.

Arch	Model	Validation				Test					
		TC	Backbone	#Params (M)	mAP (%)	F1-score (%)	Recall (%)	AUROC (%)	mAP (%)	F1-score (%)	Recall (%)
C2D Feichtenhofer et al. (2019)	8x8 R50 He et al. (2016)	23.61	27.22	12.52	10.34	82.86	29.51	8.09	6.58	83.49	
C2D NLN Feichtenhofer et al. (2019)	8x8 R50 He et al. (2016)	30.97	40.42	23.10	20.41	87.11	44.64	28.30	24.86	89.40	
I3D Carreira & Zisserman (2017)	8x8 R50 He et al. (2016)	27.33	40.93	19.78	16.93	86.44	46.41	26.37	22.25	88.79	
I3D NLN Carreira & Zisserman (2017)	8x8 R50 He et al. (2016)	34.68	41.42	24.11	23.00	86.37	47.12	28.07	24.65	88.52	
Slow Feichtenhofer et al. (2019)	8x8 R50 He et al. (2016)	31.74	40.32	21.83	19.08	84.55	45.19	26.13	22.77	88.49	
Slow Feichtenhofer et al. (2019)	4x16 R50 He et al. (2016)	31.74	42.97	22.73	19.71	85.46	46.37	28.72	25.38	88.30	
SlowFast Feichtenhofer et al. (2019)	8x8 R50 He et al. (2016)	33.76	38.76	20.29	17.66	85.91	43.02	22.63	18.98	88.51	
SlowFast Feichtenhofer et al. (2019)	4x16 R50 He et al. (2016)	33.76	37.10	17.74	14.90	84.94	42.10	23.69	20.18	87.54	
MVITv1 Fan et al. (2021)	16x4 B-CONV	36.34	17.79	7.89	6.86	72.40	12.86	5.54	4.66	74.63	
MVITv2 Li et al. (2022)	16x4 S	34.27	17.57	8.31	6.92	72.67	15.14	8.16	7.17	78.61	
X3D Feichtenhofer (2020)	13x6 S	2.02	17.59	6.63	5.63	78.27	14.07	5.77	4.52	78.23	
X3D Feichtenhofer (2020)	16x5 L	4.37	23.56	8.82	7.38	80.56	18.70	9.15	7.47	78.27	

Note: All models have been pretrained on Kinetics400 Kay et al. (2017) dataset and continually trained on MicroG-4M. TC denotes the temporal configuration (frame length  $\times$  sampling rate). #Params indicates the number of parameters (in millions, M).

Table 2: Zero-shot performance on MicroG-4M test set for models pretrained on Kinetics and fine-tuned on AVA Gu et al. (2018).

Arch	Model	TC	Backbone	Pretrain		Fine-tune	Test Result		
							mAP (%)	F1-score (%)	Recall (%)
Slow Feichtenhofer et al. (2019)	8x8 R50 He et al. (2016)		Kinetics 400 Kay et al. (2017)	AVA v2.2 Gu et al. (2018)	16.24	2.67	1.99	73.83	
SlowFast Feichtenhofer et al. (2019)	32x2 R101 He et al. (2016)		Kinetics 600 Carreira et al. (2018)	AVA v2.2 Gu et al. (2018)	23.81	6.32	6.62	77.83	

Note: All metrics are macro-averaged over action classes. mAP is measured at IoU = 0.5. F1 and AUROC are computed per class and then averaged. TC denotes the temporal configuration (frame length  $\times$  sampling rate).



Figure 3: Qualitative results for fine-grained human action recognition in microgravity, where GT denotes ground truth, MicroG-4M indicates predictions from Slow fine-tuned on MicroG-4M, and AVA denotes predictions from the same model fine-tuned on AVA. The MicroG-4M model provides more accurate predictions than its Earth-trained counterpart.

METEOR Banerjee & Lavie (2005), and BERTScore (F1) Zhang et al. (2020), all rescaled to a 0~100 range for consistency. For semantic similarity, we report S-BERT Reimers & Gurevych (2019a) and S-VQA Pathak et al. (2023) scores, both computed as cosine similarity between Sentence-BERT Reimers & Gurevych (2019b) embeddings of predicted and reference texts. S-VQA is used specifically for answer evaluation in generative visual question answering settings, capturing semantic equivalence beyond lexical overlap. More details of the implementations are delivered in the appendix.

## 5.2 RESULT ANALYSIS FOR FINE-GRAINED HUMAN ACTION RECOGNITION

We assess model performance under the setup in Sec. 5 and Sec. 3. The analysis covers three facets: (i) in-domain fine-tuning on MicroG-4M across CNN and transformer baselines; (ii) cross-domain transfer under a fixed protocol contrasting AVA  $\rightarrow$  MicroG with AVA  $\rightarrow$  JHMDB; and (iii) qualitative examinations of gravity-dependent behaviors.

### Quantitative Analysis.

We evaluate several representative models on MicroG-4M, all pretrained on Kinetics400 Kay et al. (2017) and fine-tuned on our dataset. As shown in Table 1, results plateau around 47% test mAP, indicating a substantial gap to Earth-trained regimes. The ranking also inverts common trends on Kinetics/AVA, with CNNs plus non-local modules Feichtenhofer et al. (2019); Carreira & Zisserman (2017) leading mAP/AUROC and Slow (4x16) Feichtenhofer et al. (2019) yielding the best F1, suggesting that local spatial encoding and structured receptive fields remain advantageous when motion lacks gravitational consistency. Longer temporal windows further help, highlighting the

Table 3: Cross-domain transfer under matched AVA fine-tuning (zero-shot evaluation).

Model	TC	Backbone	Test Set	mAP (%)	AUROC (%)
SlowFast Feichtenhofer et al. (2019)	32×2	R101 He et al. (2016)	JHMDB Jhuang et al. (2013)	47.50	83.98
SlowFast Feichtenhofer et al. (2019)	32×2	R101 He et al. (2016)	MicroG-4M	23.81	77.83
Slow Feichtenhofer et al. (2019)	8×8	R50 He et al. (2016)	JHMDB Jhuang et al. (2013)	34.24	76.96
Slow Feichtenhofer et al. (2019)	8×8	R50 He et al. (2016)	MicroG-4M	16.24	73.83

Table 4: Comparison of video captioning performance across open-source and closed-source models on the MicroG-4M benchmark. “#f” denotes the number of input frames used during model inference.

Model	#f	CIDEr	BLEU-4	Rouge-L	Meteor	S-BERT	BERTScore
Open-Source							
Video-ChatGPT Maaz et al. (2024)	3	0.06	0.12	10.10	4.33	39.61	85.40
mPLUG-Owl3 Ye et al. (2025)	3	0.16	0.40	11.87	5.88	47.45	85.91
LLaVA-NeXT Zhang et al. (2024)	8	0.30	1.88	16.32	14.45	54.16	84.98
Video-LLaVA Lin et al. (2024)	8	0.03	0.07	9.29	4.12	42.97	84.89
Qwen2.5-VL Qwen et al. (2025)	9	0.03	1.34	13.75	15.67	56.46	84.01
Tarsier2-Recap-7B Yuan et al. (2025)	16	0.04	0.03	0.17	0.12	51.35	84.53
InternVideo Xing et al. (2024)	90	0.77	2.60	16.57	15.18	55.28	85.41
Closed-Source							
GPT-4o Hurst et al. (2024)	6	1.74	2.65	16.46	11.27	62.18	86.75
Gemini 1.5 Pro Reid et al. (2024)	16	3.52	3.28	17.34	15.19	63.38	86.25

need for domain-adapted temporal reasoning. Under the matched transfer protocol, AVA→MicroG-4M underperforms AVA→JHMDB (Table 3), isolating a physics-driven gap beyond conventional terrestrial shifts. Comparing to AVA-finetuned models (Table 2), we observe a sharp drop when transferring directly from AVA Gu et al. (2018) to MicroG-4M despite identical pretraining/backbones; e.g., SlowFast reaches only 23.81% mAP on MicroG-4M, far below its MicroG-tuned counterpart. This indicates that Earth-trained assumptions about orientation, support/contact, and object dynamics are fragile in microgravity and are not resolved by naïve fine-tuning alone. Together, these findings position MicroG-4M as a diagnostic benchmark that surfaces gravity-dependent failure modes and motivates methods for robust, space-adapted video understanding. Our dataset thus provides a rigorous testbed for evaluating and advancing space-adapted video understanding models, especially in the context of astronaut assistance and autonomous system development.

**Qualitative Analysis.** Figure 3 presents qualitative comparisons between models trained on AVA Gu et al. (2018) and those fine-tuned on MicroG-4M, across 5 representative video clips captured inside and outside spacecraft cabins. The MicroG-4M-trained model demonstrates high alignment with ground truth labels for core actions such as “Stand”, “Walk”, and “Talk-to”, while the AVA Gu et al. (2018)-based counterpart consistently misinterprets floating or inverted postures as “Bend/Bow” or “Sit”, revealing its reliance on Earth-centric gravitational priors. A representative example in the fifth column shows the AVA Gu et al. (2018)-finetuned model misclassifying a floating astronaut as “Sit” while the MicroG-4M-trained model correctly predicts “Stand” reflecting a common correction of gravity-induced biases. Models trained on MicroG-4M also demonstrate improved robustness in distinguishing passive object drift from intentional manipulation, though semantic ambiguity remains, e.g., predicting “Carry/Hold” when a tool drifts near the astronaut’s hand without actual interaction. These results indicate that MicroG-4M mitigates terrestrial biases, enhances sensitivity to body-object dynamics, and better captures domain-specific actions, supporting future work on temporal coherence and intentionality modeling.

### 5.3 EVALUATION OF VIDEO CAPTIONING MODELS

The results in Table 4 reveal how video-language models perform on the MicroG-4M benchmark, highlighting key challenges introduced by microgravity-specific content. Lexical metrics such as CIDEr and BLEU-4 show low overall values, especially among open-source models, suggesting a significant distributional shift between MicroG-4M and typical pretraining data. The dataset’s domain-specific vocabulary, visually compositional scenes, and semantically dense annotations likely reduce surface-level overlap, which these metrics are sensitive to. In contrast, semantic similarity metrics such as S-BERT and BERTScore remain relatively higher and more consistent, indicating that several models capture the underlying intent even without lexical alignment. This underscores the semantic richness of MicroG-4M, where alternative phrasings and scientific terminology often convey similar meanings. Performance differences further reveal that input frame density and pretraining modality play key roles. InternVideo Wang et al. (2022), which processes 90 frames sampled within a 3s window, consistently outperforms other open-source models. This suggests that

Table 5: Experiments of Visual Question Answering (VQA) models on the MicroG-4M benchmark. “#f” denotes the number of input frames used during model inference.

Model	#f	CIDEr	BLEU-4	Rouge-L	Meteor	S-VQA	BERTScore
Open-Source							
LLaVA-NeXT Zhang et al. (2024)	8	24.00	22.14	15.56	12.40	38.08	87.15
Video-LLaVA Lin et al. (2024)	8	25.70	28.47	15.90	10.71	35.39	87.13
Qwen2.5-VL Qwen et al. (2025)	9	2.99	0.65	8.35	8.47	40.65	84.80
Tarsier2-Recap-7B Yuan et al. (2025)	16	5.08	0.01	0.08	0.09	29.60	85.30
Closed-Source							
Gemini 1.5 Pro Reid et al. (2024)	16	8.78	1.33	13.03	12.54	43.15	86.41
GPT-4o Hurst et al. (2024)	6	33.98	3.76	18.11	15.89	44.56	87.81

dense sampling, coupled with video-specific pretraining, enhances the model’s ability to capture subtle spatial patterns and object-scene relationships—features that are particularly important in microgravity scenarios, where visual cues are often atypical or physically ambiguous. Closed-source models, *i.e.*, GPT-4o Hurst et al. (2024) and Gemini 1.5 Pro Reid et al. (2024) achieve better scores on both lexical and semantic metrics, likely due to broader data exposure, larger capacity, or more advanced cross-modal fusion strategies. However, their relatively small performance gains further validate the challenge posed by MicroG-4M. In general, these findings position MicroG-4M as a demanding benchmark for evaluating multimodal models under domain change, highlighting the need for robust spatial reasoning, domain adaptation, and semantically aware generation strategies in unconventional environments.

#### 5.4 EVALUATION OF VISUAL QUESTION ANSWERING MODELS

The results in Table 5 demonstrate that MicroG-4M presents distinct challenges for visual question answering. Notably, there is a significant divergence between lexical and semantic evaluation metrics, particularly among open-source models. For example, Qwen2.5-VL Bai et al. (2025) yields a BLEU-4 of only 0.65 and a CIDEr score of 2.99, yet achieves the highest S-VQA score in its category (40.65). This contrast suggests that MicroG-4M questions often admit multiple semantically valid answers that differ lexically, such as paraphrased actions, scientific terms, or object references adapted to microgravity settings. This characteristic does not reflect inconsistency in evaluation, but rather underscores the conceptual and linguistic diversity embedded in the dataset. In addition, the moderate absolute scores of even the top-performing closed-source models, such as GPT-4o Hurst et al. (2024) (CIDEr 33.98, S-VQA 44.56), reveal the difficulty of reasoning over visual content in microgravity. Unlike conventional VQA datasets, MicroG-4M includes visually ambiguous cues, *e.g.*, floating objects, unusual body orientations, and tool manipulations under microgravity that challenge models trained primarily on terrestrial data. This suggests that current pretraining corpora lack sufficient coverage of such scenarios, and that purely scaling model capacity is insufficient for reliable generalization. Interestingly, increasing the number of input frames within the fixed 3s window does not consistently yield better performance. For example, Gemini 1.5 Pro Reid et al. (2024) processes 16 frames but performs worse than GPT-4o Hurst et al. (2024), which uses only 6 frames. This indicates that dense frame sampling alone is insufficient. Instead, performance depends more critically on the model’s ability to extract semantically salient cues, *e.g.*, astronaut posture, object manipulation, and spatial configurations, from visually subtle or low-motion segments. In microgravity environments, where conventional motion dynamics and object affordances are altered, effective spatial reasoning and cross-modal alignment appear to be more decisive than temporal redundancy. In summary, MicroG-4M reveals key limitations of current VQA systems in addressing domain-specific challenges, particularly those involving spatial complexity, ambiguous motion, and semantically flexible queries inherent to microgravity. Its comprehensive and specialized design establishes it as a valuable testbed for probing the robustness, adaptability, and generalization capabilities of multimodal models well beyond the scope of conventional Earth-based benchmarks.

## 6 CONCLUSION

In this work, we present MicroG-4M, the first large-scale dataset specifically curated for human action recognition and vision-language understanding in microgravity environments. The dataset features 4,759 annotated video clips with over 390,000 bounding boxes and 13,000+ action labels across 50 unique action classes. It also includes human-written captions and over 7,000 VQA pairs, enabling rich semantic understanding and reasoning. We introduce MicroG-Bench, a benchmark for

evaluating state-of-the-art models in fine-grained action recognition, video captioning, and question answering. Results show significant performance degradation in space-like settings, highlighting the need for domain-specific benchmarks and adaptation. MicroG-4M advances robust, generalizable AI for astronaut support and autonomous space operations.

## ACKNOWLEDGEMENT

The project served to prepare the SFB 1574 Circular Factory for the Perpetual Product (project ID: 471687386), approved by the German Research Foundation (DFG, German Research Foundation). This work was supported in part by the SmartAge project sponsored by the Carl Zeiss Stiftung (P2019-01-003; 2021-2026). This project is also supported in part by the National Natural Science Foundation of China under Grant No. 62473139, in part by the Hunan Provincial Research and Development Project (Grant No. 2025QK3019), and in part by the Open Research Project of the State Key Laboratory of Industrial Control Technology, China (Grant No. ICT2025B20).

## REFERENCES

Nir Aharon, Roy Orfaig, and Ben-Zion Bobrovsky. BoT-SORT: Robust associations multi-pedestrian tracking. *arXiv preprint arXiv:2206.14651*, 2022.

Mahmoud Al-Faris, John Chiverton, David Ndzi, and Ahmed Isam Ahmed. A review on computer vision-based methods for human action recognition. *Journal of Imaging*, 2020.

Saad Ali. Measuring flow complexity in videos. In *ICCV*, 2013.

Rohan Anil, Sebastian Borgeaud, Yonghui Wu, Jean-Baptiste Alayrac, Jiahui Yu, Radu Soricut, Johan Schalkwyk, Andrew M. Dai, Anja Hauth, Katie Millican, David Silver, Slav Petrov, Melvin Johnson, Ioannis Antonoglou, Julian Schrittwieser, Amelia Glaese, Jilin Chen, Emily Pitler, Timothy P. Lillicrap, Angeliki Lazaridou, Orhan Firat, James Molloy, Michael Isard, Paul Ronald Barham, Tom Hennigan, Benjamin Lee, Fabio Viola, Malcolm Reynolds, Yuanzhong Xu, Ryan Doherty, Eli Collins, Clemens Meyer, Eliza Rutherford, Erica Moreira, Kareem Ayoub, Megha Goel, George Tucker, Enrique Piqueras, Maxim Krikun, Iain Barr, Nikolay Savinov, Ivo Danihelka, Becca Roelofs, Anaïs White, Anders Andreassen, Tamara von Glehn, Lakshman Yagati, Mehran Kazemi, Lucas Gonzalez, Misha Khalman, Jakub Sygnowski, et al. Gemini: family of highly capable multimodal models. *arXiv preprint arXiv:2312.11805*, 2023.

Christopher Assad, Michael Wolf, Adrian Stoica, Theodoros Theodoridis, and Kyrre Glette. BioSleeve: A natural EMG-based interface for HRI. In *HRI*, 2013.

Shuai Bai, Keqin Chen, Xuejing Liu, Jialin Wang, Wenbin Ge, Sibo Song, Kai Dang, Peng Wang, Shijie Wang, Jun Tang, Humen Zhong, Yuanzhi Zhu, Mingkun Yang, Zhaohai Li, Jianqiang Wan, Pengfei Wang, Wei Ding, Zheren Fu, Yiheng Xu, Jiabo Ye, Xi Zhang, Tianbao Xie, Zesen Cheng, Hang Zhang, Zhibo Yang, Haiyang Xu, and Junyang Lin. Qwen2.5-VL technical report. *arXiv preprint arXiv:2502.13923*, 2025.

Satanjeev Banerjee and Alon Lavie. METEOR: An automatic metric for MT evaluation with improved correlation with human judgments. In *IEEvaluation@ACL*, 2005.

Fabian Caba Heilbron, Victor Escorcia, Bernard Ghanem, and Juan Carlos Niebles. ActivityNet: A large-scale video benchmark for human activity understanding. In *CVPR*, 2015.

Fernando Camarena, Miguel Gonzalez-Mendoza, Leonardo Chang, and Ricardo Cuevas-Ascencio. An overview of the vision-based human action recognition field. *MCA*, 2023.

Joao Carreira and Andrew Zisserman. Quo vadis, action recognition? A new model and the kinetics dataset. In *CVPR*, 2017.

Joao Carreira, Eric Noland, Andras Banki-Horvath, Chloe Hillier, and Andrew Zisserman. A short note about kinetics-600. *arXiv preprint arXiv:1808.01340*, 2018.

David L. Chen and William B. Dolan. Collecting highly parallel data for paraphrase evaluation. In *ACL*, 2011.

Lin Chen, Xilin Wei, Jinsong Li, Xiaoyi Dong, Pan Zhang, Yuhang Zang, Zehui Chen, Haodong Duan, Lin Bin, Zhenyu Tang, Li Yuan, Yu Qiao, Dahua Lin, Feng Zhao, and Jiaqi Wang. ShareGPT4Video: Improving video understanding and generation with better captions. In *NeurIPS*, 2024.

Shizhe Chen, Yuqing Song, Yida Zhao, Qin Jin, Zhaoyang Zeng, Bei Liu, Jianlong Fu, and Alexander G. Hauptmann. Activitynet 2019 task 3: Exploring contexts for dense captioning events in videos. *arXiv preprint arXiv:1907.05092*, 2019.

Jihoon Chung, Cheng-hsin Wuu, Hsuan-ru Yang, Yu-Wing Tai, and Chi-Keung Tang. HAA500: Human-centric atomic action dataset with curated videos. In *ICCV*, 2021.

Holly Dinkel, Julia Di, Jamie Santos, Keenan Albee, Paulo VK Borges, Marina Moreira, Ryan Soussan, Oleg Alexandrov, Brian Coltin, and Trey Smith. AstrobeeCD: Change detection in microgravity with free-flying robots. *Acta Astronautica*, 2024.

Till Eisenberg, Gerhard Reichert, Ralf Christe, and Judith Irina Buchheim. Assistant in space. *Aerospace Psychology and Human Factors: Applied Methods and Techniques*, 2024.

Haoqi Fan, Bo Xiong, Karttikeya Mangalam, Yanghao Li, Zhicheng Yan, Jitendra Malik, and Christoph Feichtenhofer. Multiscale vision transformers. In *ICCV*, 2021.

Christoph Feichtenhofer. X3D: Expanding architectures for efficient video recognition. In *CVPR*, 2020.

Christoph Feichtenhofer, Haoqi Fan, Jitendra Malik, and Kaiming He. SlowFast networks for video recognition. In *ICCV*, 2019.

Shuwei Gan, Xiaohu Zhang, Sheng Zhuge, Chenghao Ning, Lijun Zhong, and You Li. A multi-view vision system for astronaut postural reconstruction with self-calibration. *Aerospace*, 2023.

Qing Gao, Jinguo Liu, and Zhaojie Ju. Robust real-time hand detection and localization for space human–robot interaction based on deep learning. *Neurocomputing*, 2020.

Yash Goyal, Tejas Khot, Douglas Summers-Stay, Dhruv Batra, and Devi Parikh. Making the V in VQA matter: Elevating the role of image understanding in visual question answering. In *CVPR*, 2017.

Alexey Gritsenko, Xuehan Xiong, Josip Djolonga, Mostafa Dehghani, Chen Sun, Mario Lučić, Cordelia Schmid, and Anurag Arnab. End-to-end spatio-temporal action localisation with video transformers. *arXiv preprint arXiv:2304.12160*, 2023.

Chunhui Gu, Chen Sun, David A. Ross, Carl Vondrick, Caroline Pantofaru, Yeqing Li, Sudheendra Vijayanarasimhan, George Toderici, Susanna Ricco, Rahul Sukthankar, Cordelia Schmid, and Jitendra Malik. AVA: A video dataset of spatio-temporally localized atomic visual actions. In *CVPR*, 2018.

Shota Hagio, Akihiko Ishihara, Masahiro Terada, Hiroko Tanabe, Benio Kibushi, Akira Higashibata, Shin Yamada, Satoshi Furukawa, Chiaki Mukai, Noriaki Ishioka, and Motoki Kouzaki. Muscle synergies of multidirectional postural control in astronauts on earth after a long-term stay in space. *Journal of Neurophysiology*, 2022.

Kaiming He, Xiangyu Zhang, Shaoqing Ren, and Jian Sun. Deep residual learning for image recognition. In *CVPR*, 2016.

Michael Heilman and Noah A. Smith. Question generation via overgenerating transformations and ranking. *DTIC Document*, 2009.

Yushi Hu, Hang Hua, Zhengyuan Yang, Weijia Shi, Noah A Smith, and Jiebo Luo. PromptCap: Prompt-guided image captioning for VQA with GPT-3. In *ICCV*, 2023.

Aaron Hurst, Adam Lerer, Adam P. Goucher, Adam Perelman, Aditya Ramesh, Aidan Clark, AJ Os-trow, Akila Welihinda, Alan Hayes, Alec Radford, Aleksander Madry, Alex Baker-Whitcomb, Alex Beutel, Alex Borzunov, Alex Carney, Alex Chow, Alex Kirillov, Alex Nichol, Alex Paino, Alex Renzin, Alex Tachard Passos, Alexander Kirillov, Alexi Christakis, Alexis Conneau, Ali Kamali, Allan Jabri, Allison Moyer, Allison Tam, Amadou Crookes, Amin Tootoonchian, Ananya Kumar, Andrea Vallone, Andrej Karpathy, Andrew Braunstein, Andrew Cann, Andrew Codispoti, Andrew Galu, Andrew Kondrich, Andrew Tulloch, Andrey Mishchenko, Angela Baek, Angela Jiang, Antoine Pelisse, Antonia Woodford, Anuj Gosalia, Arka Dhar, Ashley Pantuliano, Avi Nayak, Avital Oliver, Barret Zoph, Behrooz Ghorbani, Ben Leimberger, Ben Rossen, Ben Sokolowsky, Ben Wang, Benjamin Zweig, Beth Hoover, Blake Samic, Bob McGrew, Bobby Spero, Bogo Giertler, Bowen Cheng, Brad Lightcap, Brandon Walkin, Brendan Quinn, Brian Guarraci, Brian Hsu, Bright Kellogg, Brydon Eastman, Camillo Lugaresi, Carroll L. Wainwright, Cary Bassin, Cary Hudson, Casey Chu, Chad Nelson, Chak Li, Chan Jun Shern, Channing Conger, Charlotte Barette, Chelsea Voss, Chen Ding, Cheng Lu, Chong Zhang, Chris Beaumont, Chris Hallacy, Chris Koch, Christian Gibson, Christina Kim, Christine Choi, Christine McLeavey, Christopher Hesse, Claudia Fischer, Clemens Winter, Coley Czarnecki, Colin Jarvis, Colin Wei, Constantin Koumouzelis, and Dane Sherburn. GPT-4o system card. *arXiv preprint arXiv:2410.21276*, 2024.

Yunseok Jang, Yale Song, Youngjae Yu, Youngjin Kim, and Gunhee Kim. Tgif-qa: Toward spatio-temporal reasoning in visual question answering. In *CVPR*, 2017.

Sylvie Jeannin and Ajay Divakaran. MPEG-7 visual motion descriptors. *IEEE Transactions on Circuits and Systems for Video Technology*, 2001.

H Jhuang, J Gall, S Zuffi, C Schmid, and MJ Black. Joint-annotated human motion data base, 2013.

Justin Johnson, Bharath Hariharan, Laurens van der Maaten, Li Fei-Fei, C. Lawrence Zitnick, and Ross B. Girshick. CLEVR: A diagnostic dataset for compositional language and elementary visual reasoning. In *CVPR*, 2017.

Suyoung Kang, Ryan Soussan, Daekyeong Lee, Brian Coltin, Andres Mora Vargas, Marina Moreira, Katie Browne, Ruben Garcia, Maria Bualat, Trey Smith, Jonathan Barlow, Jose Benavides, Eunju Jeong, and Pyojin Kim. Astrobee ISS free-flyer datasets for space intra-vehicular robot navigation research. *RA-L*, 2024.

Will Kay, João Carreira, Karen Simonyan, Brian Zhang, Chloe Hillier, Sudheendra Vijayanarasimhan, Fabio Viola, Tim Green, Trevor Back, Paul Natsev, Mustafa Suleyman, and Andrew Zisserman. The kinetics human action video dataset. *arXiv preprint arXiv:1705.06950*, 2017.

Rahima Khanam and Muhammad Hussain. YOLOv11: An overview of the key architectural enhancements. *arXiv preprint arXiv:2410.17725*, 2024.

Ranjay Krishna, Kenji Hata, Frederic Ren, Li Fei-Fei, and Juan Carlos Niebles. Dense-captioning events in videos. In *ICCV*, 2017.

Hildegard Kuehne, Hueihan Jhuang, Estíbaliz Garrote, Tomaso Poggio, and Thomas Serre. HMDB: A large video database for human motion recognition. In *ICCV*, 2011.

Viet-Tuan Le, Kiet Tran-Trung, and Vinh Truong Hoang. A comprehensive review of recent deep learning techniques for human activity recognition. *CIN*, 2022.

Jie Lei, Licheng Yu, Mohit Bansal, and Tamara L. Berg. TVQA: Localized, compositional video question answering. In *EMNLP*, 2018.

Feng Li, Renrui Zhang, Hao Zhang, Yuanhan Zhang, Bo Li, Wei Li, Zejun Ma, and Chunyuan Li. LLaVA-NeXT-Interleave: Tackling multi-image, video, and 3D in large multimodal models. *arXiv preprint arXiv:2407.07895*, 2024.

Kunchang Li, Yinan He, Yi Wang, Yizhuo Li, Wenhui Wang, Ping Luo, Yali Wang, Limin Wang, and Yu Qiao. VideoChat: Chat-centric video understanding. *arXiv preprint arXiv:2305.06355*, 2023.

Yanghao Li, Chao-Yuan Wu, Haoqi Fan, Karttikeya Mangalam, Bo Xiong, Jitendra Malik, and Christoph Feichtenhofer. MViTv2: Improved multiscale vision transformers for classification and detection. In *CVPR*, 2022.

Bin Lin, Yang Ye, Bin Zhu, Jiaxi Cui, Munan Ning, Peng Jin, and Li Yuan. Video-LLaVA: Learning united visual representation by alignment before projection. In *EMNLP*, 2024.

Chin-Yew Lin. Rouge: A package for automatic evaluation of summaries. In *Text Summarization Branches Out*, 2004.

Gu Lingyun, Zhang Lin, and Wang Zhaokui. Hierarchical attention-based astronaut gesture recognition: A dataset and cnn model. *IEEE Access*, 2020.

Muhammad Maaz, Hanoona Rasheed, Salman Khan, and Fahad Khan. Video-ChatGPT: Towards detailed video understanding via large vision and language models. In *ACL*, 2024.

Luisa Mao, Ryan Soussan, Brian Coltin, Trey Smith, and Joydeep Biswas. Semantic masking and visual feature matching for robust localization. In *iSpaRo*, 2024.

Ian D Miller, Ryan Soussan, Brian Coltin, Trey Smith, and Vijay Kumar. Robust semantic mapping and localization on a free-flying robot in microgravity. In *ICRA*, 2022.

Clara Moskowitz and Zane Wolf. The astronaut club. *Scientific American*, 332(2):88, February 2025. doi: 10.1038/scientificamerican022025-LZ8uxT6kydMF8ej8rDLA4.

Charles Oestreich, Antonio Terán Espinoza, Jessica Todd, Keenan Albee, and Richard Linares. On-orbit inspection of an unknown, tumbling target using NASA's astrobee robotic free-flyers. In *CVPR*, 2021.

Jingxuan Ouyang, Wentao Xie, Guangsheng Xu, Chujun Li, Shuwei Gan, Xiaohu Zhang, Xia Yang, Changhua Jiang, et al. SpacesuitPose: Deep learning-based spacesuit pose estimation in extravehicular activities from monocular images. *Acta Astronautica*, 2025.

Kishore Papineni, Salim Roukos, Todd Ward, and Wei-Jing Zhu. Bleu: a method for automatic evaluation of machine translation. In *ACL*, 2002.

Preksha Pareek and Ankit Thakkar. A survey on video-based human action recognition: recent updates, datasets, challenges, and applications. *AIR*, 2021.

Sanchit Pathak, Garima Singh, Ashish Anand, and Prithwijit Guha. S-VQA: Sentence-based visual question answering. In *ICVGIP*, 2023.

Kunyu Peng, Alina Roitberg, Kailun Yang, Jiaming Zhang, and Rainer Stiefelhagen. Transdarc: Transformer-based driver activity recognition with latent space feature calibration. In *IROS*, 2022.

Qwen, An Yang, Baosong Yang, Beichen Zhang, Binyuan Hui, Bo Zheng, Bowen Yu, Chengyuan Li, Dayiheng Liu, Fei Huang, Haoran Wei, Huan Lin, Jian Yang, Jianhong Tu, Jianwei Zhang, Jianxin Yang, Jiaxi Yang, Jingren Zhou, Junyang Lin, Kai Dang, Keming Lu, Keqin Bao, Kexin Yang, Le Yu, Mei Li, Mingfeng Xue, Pei Zhang, Qin Zhu, Rui Men, Runji Lin, Tianhao Li, Tianyi Tang, Tingyu Xia, Xingzhang Ren, Xuancheng Ren, Yang Fan, Yang Su, Yichang Zhang, Yu Wan, Yuqiong Liu, Zeyu Cui, Zhenru Zhang, and Zihan Qiu. Qwen2.5 technical report, 2025. URL <https://arxiv.org/abs/2412.15115>.

Machel Reid, Nikolay Savinov, Denis Teplyashin, Dmitry Lepikhin, Timothy P. Lillicrap, Jean-Baptiste Alayrac, Radu Soricut, Angeliki Lazaridou, Orhan Firat, Julian Schrittwieser, Ioannis Antonoglou, Rohan Anil, Sebastian Borgeaud, Andrew M. Dai, Katie Millican, Ethan Dyer, Mia Glaese, Thibault Sottiaux, Benjamin Lee, Fabio Viola, Malcolm Reynolds, Yuanzhong Xu, James Molloy, Jilin Chen, Michael Isard, Paul Barham, Tom Hennigan, Ross McIlroy, Melvin Johnson, Johan Schalkwyk, Eli Collins, Eliza Rutherford, Erica Moreira, Kareem Ayoub, Megha Goel, Clemens Meyer, Gregory Thornton, Zhen Yang, Henryk Michalewski, Zaheer Abbas, Nathan Schucher, Ankesh Anand, Richard Ives, James Keeling, Karel Lenc, Salem Haykal, Siamak Shakeri, Pranav Shyam, Aakanksha Chowdhery, Roman Ring, Stephen Spencer, Eren Sezener, et al. Gemini 1.5: Unlocking multimodal understanding across millions of tokens of context. *arXiv preprint arXiv:2403.05530*, 2024.

Nils Reimers and Iryna Gurevych. Sentence-BERT: Sentence embeddings using siamese BERT-networks. In *EMNLP/IJCNLP*, 2019a.

Nils Reimers and Iryna Gurevych. Sentence-bert: Sentence embeddings using siamese bert-networks. *arXiv preprint arXiv:1908.10084*, 2019b.

Chaitanya Ryali, Yuan-Ting Hu, Daniel Bolya, Chen Wei, Haoqi Fan, Po-Yao Huang, Vaibhav Aggarwal, Arkabandhu Chowdhury, Omid Poursaeed, Judy Hoffman, Jitendra Malik, Yanghao Li, and Christoph Feichtenhofer. Hiera: A hierarchical vision transformer without the bells-and-whistles. In *ICML*, 2023.

Dian Shao, Yue Zhao, Bo Dai, and Dahua Lin. FineGym: A hierarchical video dataset for fine-grained action understanding. In *CVPR*, 2020.

Khurram Soomro, Amir Roshan Zamir, and Mubarak Shah. UCF101: A dataset of 101 human actions classes from videos in the wild. *arXiv preprint arXiv:1212.0402*, 2012.

Ryan Soussan, Varsha Kumar, Brian Coltin, and Trey Smith. Astroloc: An efficient and robust localizer for a free-flying robot. In *ICRA*, 2022.

Richard Szeliski. *Computer Vision: Algorithms and Applications*. Springer-Verlag, Berlin, Heidelberg, 1st edition, 2010. ISBN 1848829345.

Makarand Tapaswi, Yukun Zhu, Rainer Stiefelhagen, Antonio Torralba, Raquel Urtasun, and Sanja Fidler. MovieQA: Understanding stories in movies through question-answering. In *CVPR*, 2016.

Brent E. Tweddele, Alvar Saenz-Otero, John J. Leonard, and David W. Miller. Factor graph modeling of rigid-body dynamics for localization, mapping, and parameter estimation of a spinning object in space. *JFR*, 2015.

Ramakrishna Vedantam, C. Lawrence Zitnick, and Devi Parikh. CIDEr: Consensus-based image description evaluation. In *CVPR*, 2015.

Limin Wang, Bingkun Huang, Zhiyu Zhao, Zhan Tong, Yinan He, Yi Wang, Yali Wang, and Yu Qiao. VideoMAE V2: Scaling video masked autoencoders with dual masking. In *CVPR*, 2023a.

Rui Wang, Dongdong Chen, Zuxuan Wu, Yinpeng Chen, Xiyang Dai, Mengchen Liu, Lu Yuan, and Yu-Gang Jiang. Masked video distillation: Rethinking masked feature modeling for self-supervised video representation learning. In *CVPR*, 2023b.

Xin Wang, Jiawei Wu, Junkun Chen, Lei Li, Yuan-Fang Wang, and William Yang Wang. VaTeX: A large-scale, high-quality multilingual dataset for video-and-language research. In *ICCV*, 2019.

Yi Wang, Kunchang Li, Yizhuo Li, Yinan He, Bingkun Huang, Zhiyu Zhao, Hongjie Zhang, Jilan Xu, Yi Liu, Zun Wang, Sen Xing, Guo Chen, Junting Pan, Jiashuo Yu, Yali Wang, Limin Wang, and Yu Qiao. InternVideo: General video foundation models via generative and discriminative learning. *arXiv preprint arXiv:2212.03191*, 2022.

Junbin Xiao, Xindi Shang, Angela Yao, and Tat-Seng Chua. NExT-QA: Next phase of question-answering to explaining temporal actions. In *CVPR*, 2021.

Zhen Xing, Qijun Feng, Haoran Chen, Qi Dai, Han Hu, Hang Xu, Zuxuan Wu, and Yu-Gang Jiang. A survey on video diffusion models. *ACM Computing Surveys*, 2024.

Dejing Xu, Zhou Zhao, Jun Xiao, Fei Wu, Hanwang Zhang, Xiangnan He, and Yueting Zhuang. Video question answering via gradually refined attention over appearance and motion. In *ACM Multimedia*, 2017.

Jun Xu, Tao Mei, Ting Yao, and Yong Rui. MSR-VTT: A large video description dataset for bridging video and language. In *CVPR*, 2016.

Hui Yang, Lekha Chaisorn, Yunlong Zhao, Shi-Yong Neo, and Tat-Seng Chua. Videoqa: question answering on news video. In *Proceedings of the eleventh ACM international conference on Multimedia*, pp. 632–641, 2003.

Jiabo Ye, Haiyang Xu, Haowei Liu, Anwen Hu, Ming Yan, Qi Qian, Ji Zhang, Fei Huang, and Jingren Zhou. mPLUG-Owl3: Towards long image-sequence understanding in multi-modal large language models. In *ICLR*, 2025.

Kexin Yi, Chuang Gan, Yunzhu Li, Pushmeet Kohli, Jiajun Wu, Antonio Torralba, and Joshua B. Tenenbaum. CLEVRER: Collision events for video representation and reasoning. In *ICLR*, 2020.

Zhou Yu, Dejing Xu, Jun Yu, Ting Yu, Zhou Zhao, Yueting Zhuang, and Dacheng Tao. ActivityNet-QA: A dataset for understanding complex web videos via question answering. In *AAAI*, 2019.

Liping Yuan, Jiawei Wang, Haomiao Sun, Yuchen Zhang, and Yuan Lin. Tarsier2: Advancing large vision-language models from detailed video description to comprehensive video understanding. *arXiv preprint arXiv:2501.07888*, 2025.

Tianyi Zhang, Varsha Kishore, Felix Wu, Kilian Q. Weinberger, and Yoav Artzi. BERTScore: Evaluating text generation with BERT. In *ICLR*, 2020.

Yuanhan Zhang, Jinming Wu, Wei Li, Bo Li, Zejun Ma, Ziwei Liu, and Chunyuan Li. Video instruction tuning with synthetic data. *arXiv preprint arXiv:2410.02713*, 2024.

Luowei Zhou, Chenliang Xu, and Jason Corso. Towards automatic learning of procedures from web instructional videos. In *AAAI*, 2018.

## APPENDIX

### A TECHNICAL LIMITATIONS

MicroG-4M introduces the first unified benchmark for high-level video understanding in microgravity environments, but several technical limitations remain that could guide future refinement and expansion.

One challenge lies in the ambiguity and subjectivity of annotations. Interpreting actions and generating captions can vary between annotators, especially in visually ambiguous frames or when inference is required. Even with cross-validation protocols in place, some degree of subjectivity may persist, introducing annotation noise.

Another limitation is the restricted temporal context. Each video clip spans only three seconds, which may hinder the ability to model long-term dependencies. This limitation is particularly relevant when modeling multi-step operations that are common in space missions.

The dataset is currently limited to RGB visual input, which constrains the potential for multimodal understanding. Future versions could benefit from the inclusion of additional modalities such as audio signals or communication transcripts to support more comprehensive reasoning.

There is also an inherent domain bias introduced by the inclusion of cinematic footage. While these clips are visually high-fidelity and physically plausible, they may differ in visual style and narrative framing from real operational recordings. This discrepancy can affect the generalizability of models trained on the dataset.

Finally, the scale and annotation coverage of the dataset present further constraints. The current release offers a carefully annotated subset of the full video collection, suitable for benchmarking, but smaller than many large-scale web datasets. Continued annotation efforts are underway to expand the dataset, covering a wider range of clips, actions, and scene types to support more diverse downstream applications, including temporal reasoning and sequence-level inference.

### B POTENTIAL SOCIAL IMPACTS

MicroG-4M introduces the first benchmark specifically designed for video understanding and vision-language reasoning in microgravity environments. It comprises 4,759 curated clips supporting fine-grained action recognition, video captioning, and visual question answering. These tasks collectively provide a testbed for evaluating models under the unique motion dynamics and spatial ambiguities posed by microgravity.

While MicroG-4M is not intended for deployment, it may inform downstream research in areas such as astronaut behavior modeling, procedural understanding, or human–robot collaboration. Its vision-language annotations also facilitate studies on video summarization and temporal grounding, with potential implications for future human-AI interfaces in space-based or analog settings.

MicroG-4M enables the analysis of model limitations under microgravity-specific challenges, such as sensitivity to gravitational priors and orientation ambiguity, offering a foundation for research on robustness and generalization. Although developed for space-based contexts, the dataset’s motion and interaction patterns may inspire comparative studies in gravity-reduced analog environments, such as underwater settings.

Furthermore, the semantic complexity of the captioning and QA tasks highlights challenges including hallucination and semantic inconsistency, positioning MicroG-4M as a testbed for evaluating the reliability and grounding of multimodal models in physically unfamiliar conditions.

### C SAFETY AND ETHICAL DISCUSSION

MicroG-4M is developed as a research-oriented benchmark for video understanding in microgravity environments. While ethical standards were followed throughout its construction, several considerations are noted to promote responsible and informed use.

All real-world videos are sourced from publicly available materials released by official space agencies and educational institutions, containing no private or sensitive content. Astronauts are shown exclusively in professional contexts. Simulated cinematic content, while enriching visual diversity, may introduce stylistic bias that differs from real operational footage.

All captions and QA annotations were created manually by annotators with domain guidance. LLMs were employed exclusively for grammatical correction and fluency enhancement, without contributing to semantic generation. Nonetheless, users should remain aware of any residual stylistic biases introduced during this refinement process.

MicroG-4M is intended solely for non-commercial academic research. It is not validated for real-world deployment, particularly in sensitive domains such as surveillance or defense. Users are advised to evaluate generalization carefully and avoid overextension of model outputs.

We encourage community feedback on potential biases, content issues, or safety risks. Future versions will include expanded validation and filtering to enhance transparency and data quality.

## D ADDITIONAL QUALITATIVE ANALYSIS

### D.1 FINE-GRAINED HUMAN ACTION RECOGNITION

We provide qualitative comparisons using representative video samples to illustrate the fine-grained action recognition performance of different models in microgravity scenarios (Figure 4).

The AVA fine-tuned model frequently misinterprets microgravity-specific postures and contexts, exhibiting errors such as misclassifying hatch-crossing as bend/bow or generating unrealistic predictions like detecting a “smoke” action. In contrast, the MicroG-4M fine-tuned models demonstrate improved accuracy by correctly identifying nuanced and compound actions specific to microgravity environments, as illustrated by the more precise recognition of actions like carry/hold, lift/pickup, and put on/off clothing. The highest-performing MicroG-4M model (I3D Non-local) further reduces both false positives and missed detections, highlighting its superior capability in recognizing complex and subtle astronaut activities.

These examples underscore the necessity for specialized training data, such as MicroG-4M, to effectively capture and recognize fine-grained human actions unique to microgravity conditions.

### D.2 VIDEO CAPTIONING

We provide qualitative examples to emphasize the unique challenges posed by space-related scenarios and the limitations of existing state-of-the-art multimodal models (mPLUG-Owl13, LLaVA-NeXT, GPT-4o, Gemini 1.5 Pro) in accurately capturing specialized details inherent to space station environments.

In the first scenario (Figure 5, left), all models demonstrate significant shortcomings in capturing critical, astronaut-specific information and precise operational context, underscoring the difficulty in accurately describing space-station activities without access to specialized annotations.

The second scenario (Figure 5, right) represents a relatively simpler context, yet models still lack precise details and fail to fully leverage the specialized information present in our ground-truth annotations. These examples illustrate the inherent difficulty in accurately modeling highly specialized and contextually rich scenarios typical of space environments, highlighting the necessity and distinctive value of our carefully annotated space-oriented dataset.

Overall, these qualitative results demonstrate the critical importance of domain-specific annotation for effectively capturing the nuanced details and specialized context essential in space exploration scenarios.

### D.3 VIDEO QUESTION ANSWERING

We present qualitative examples illustrating the performance of state-of-the-art multimodal models (Gemini 1.5 Pro, GPT-4o, Video-LLaVA) on challenging Video Question-Answering (VQA) tasks specifically related to space environments.

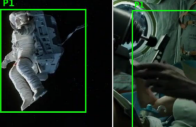
Key Frame					
Ground Truth	walk, enter, touch talk to	stand, carry/hold talk to, put down put on/off clothing	carry/hold	stand	sit operate spaceship
AVA SLOW	walk, enter, touch talk to <b>bend/bow</b>	stand, carry/hold talk to, put down put on/off clothing	carry/hold <b>sit smoke</b>	stand	sit operate spaceship <b>lie/sleep, carry/hold</b>
MicroG-4M SLOW	walk, enter, touch talk to	stand, carry/hold talk to, put down put on/off clothing	carry/hold	stand	sit operate spaceship <b>carry/hold</b>
MicroG-4M I3D NLN	walk, enter, touch talk to	stand, carry/hold talk to, put down put on/off clothing <b>lift/pickup</b>	carry/hold <b>talk to</b>	stand	sit operate spaceship

Figure 4: Qualitative results for fine-grained human action recognition in microgravity. Below the frame samples, the first row presents the ground truth labels of the actions. The second row presents the predictions of the Slow architecture fine-tuned on the AVA dataset. The third row shows the predictions of the Slow architecture fine-tuned on the MicroG-4M dataset. The last row shows the predictions of the I3D Non-Local Network (NLN) architecture fine-tuned on MicroG-4M. For both the Slow and I3D NLN architectures, the AVA and MicroG-4M models were trained under the same configuration: a ResNet-50 backbone with an 8x8 input (frame length x sampling rate), pre-trained on Kinetics-400. The I3D NLN model fine-tuned on MicroG-4M achieved the highest mAP among our baselines. Gray text denotes missed detections, while red text denotes false detections.

	
<b>Ground Truth</b>	<b>Caption Length: 93</b>
NASA astronaut Steven Swanson wears a charcoal-gray T-shirt, dark blue utility trousers with reflective strips and a blue belt; he leans toward the <b>open crew-quarter</b> on his right, grips the doorway's blue handle with his left hand, and points his iPad-holding right hand inside while talking. A blue work bench is visible in background, an overhead PCS screen glows with green status blocks, and the forward hatch farther aft is criss-crossed with bungee cords that secure white cargo bags	
<b>mPLUG-Owl3</b>	<b>Caption Length: 18</b>
A man in a space suit is floating in a space station, reaching out to a panel and interacting with it.	
<b>LLaVA-NeXT</b>	<b>Caption Length: 183</b>
In the video, we see a man inside a spacecraft, which appears to be a part of the International Space Station (ISS). The man is wearing a white shirt and blue pants, and he is standing in front of a control panel with various buttons and switches. He seems to be in the process of operating the controls, possibly adjusting something or preparing for a task. The spacecraft is filled with various pieces of equipment and screens, indicating a complex and technologically advanced environment. The man's posture suggests he is focused and engaged in his work. The background is filled with the typical interior of a spacecraft, with white walls and panels, and there are multiple screens and buttons, suggesting a high level of technology and functionality. The lighting is bright, typical of a space environment, and the overall atmosphere is one of concentration and purpose. The man's actions and the setting suggest that he is performing a task that is crucial to the operation of the spacecraft.	
<b>GPT-4o</b>	<b>Caption Length: 53</b>
The video shows an astronaut inside a space station module. He is interacting with a storage compartment, opening and inspecting it. The environment is filled with various cables, equipment, and a monitor displaying information. The astronaut moves carefully, likely due to the microgravity conditions.	
<b>Gemini 1.5 Pro</b>	<b>Caption Length: 92</b>
The video shows a man inside what looks like a spacecraft. He wears a dark gray short-sleeved t-shirt, dark blue shorts, and dark gray compression sleeves on his lower legs. He's working on a white, padded, box-like structure with a door that opens outward. He closes the door partway, then further adjusts something inside near the opening. A computer monitor is visible in the background behind his right shoulder, and various pieces of equipment are visible throughout the shot.	
<b>Ground Truth</b>	<b>Caption Length: 60</b>
In the video, NASA astronaut Suni Williams is stationed in <b>Node 3 module</b> , wearing a black T-shirt and shorts. She is secured to the <b>treadmill</b> using a <b>white harness system</b> featuring elastic cords and locking chains to counteract microgravity forces. The background reveals an array of equipment and control panels neatly arranged along the walls, emphasizing the station's high-tech operational environment.	
<b>mPLUG-Owl3</b>	<b>Caption Length: 18</b>
A person is seen floating in a space station, wearing a harness and moving around in a zero-gravity environment.	
<b>LLaVA-NeXT</b>	<b>Caption Length: 167</b>
The video depicts a person engaging in a physical activity within a confined space that appears to be a simulated or controlled environment, possibly a gym or a space station. The individual is wearing a harness and is seen running on a treadmill, suggesting a focus on cardiovascular exercise. The setting is well-lit, with a mix of white and blue walls and equipment, indicating a modern and possibly scientific or technological context. The person's attire consists of a black top and blue shorts, and they are barefoot, which is common in gym settings for comfort and safety. The camera angle is from a side perspective, capturing the person's profile as they run, emphasizing the movement and the harness's support. The lighting is bright, and the overall atmosphere is clinical and controlled, which is typical for a space designed for physical training or research.	
<b>GPT-4o</b>	<b>Caption Length: 63</b>
The video shows an astronaut running on a treadmill inside a space station. They are wearing a harness to stay attached to the treadmill due to the microgravity environment. The astronaut is exercising, which is crucial for maintaining health during space missions. The surroundings are filled with equipment and instruments typical of a space station.	
<b>Gemini 1.5 Pro</b>	<b>Caption Length: 151</b>
The video shows an astronaut running on a treadmill aboard the International Space Station (ISS). The astronaut is wearing a black t-shirt, blue shorts, and a white harness that attaches them to the treadmill. This prevents them from floating away in the microgravity environment. The treadmill appears to be in a relatively narrow passageway within the ISS. The walls around the treadmill are metallic and white, with various pieces of equipment and wiring visible. A folded-up white object, possibly bedding, can be seen in the background. Blue support structures are visible at the sides of the frame. The astronaut is running with a steady pace, their hair slightly tousled from the movement. Their concentration suggests they are engaged in a physical exercise routine.	

Figure 5: Qualitative examples illustrating ground-truth captions and outputs from four state-of-the-art multimodal models. The left example represents a challenging scenario, in which all models fail to accurately capture detailed and precise information. The right example demonstrates a relatively simpler scenario, where model-generated captions exhibit closer alignment to the ground truth. Each caption includes the corresponding caption length (in words), with key details highlighted in the ground-truth captions.

The provided examples (Figure 6) showcase diverse and challenging scenarios uniquely associated with space-based contexts. The top-left example demonstrates the complexity of accurately inter-

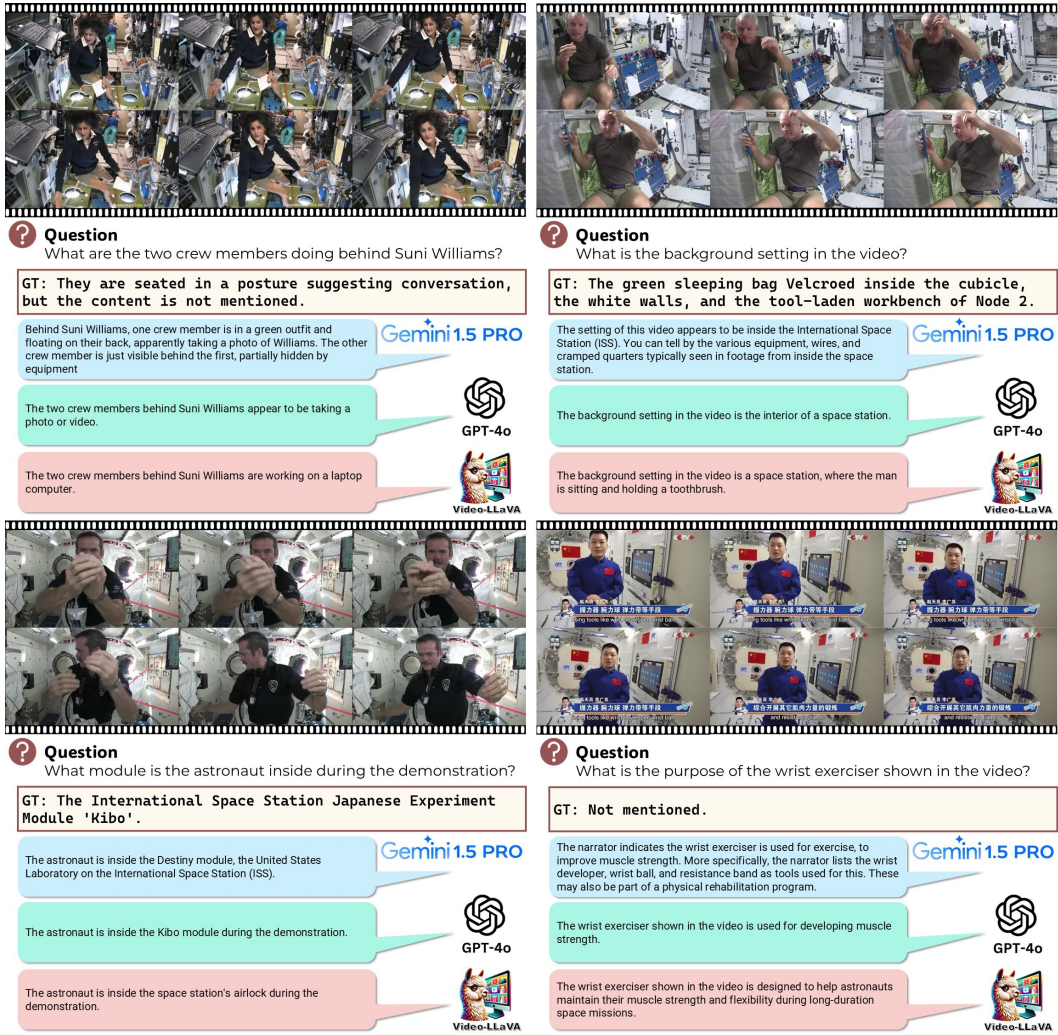


Figure 6: Qualitative examples illustrating Ground-Truth (GT) answers and corresponding responses generated by three state-of-the-art multimodal models.

preting multiple astronauts’ actions within confined spaces, especially when occlusions occur. The bottom-left example emphasizes challenges in accurately identifying specific locations unique to space environments. The top-right scenario tests models’ abilities to describe various specialized objects within densely detailed backgrounds, typical of spacecraft interiors. Lastly, the bottom-right example addresses the models’ propensity for hallucination by evaluating their capacity to accurately infer details not explicitly mentioned in the visual content.

Overall, these qualitative analyses highlight significant limitations of current multimodal models in handling space-specific scenarios, underscoring the critical need for detailed and specialized annotations provided by our dataset to enhance performance and robustness in space-related VQA tasks.

## E DATA FORMAT CONVERSION

To simplify frame-level annotation processing, we adapted our dataset to match the AVA format, with one modification: using frame stamps rather than timestamps. This allows direct frame indexing, aligning better with our annotation scheme and reducing unnecessary conversion overhead.

## E.1 DATASET METADATA

Our dataset metadata is structured hierarchically into two categories—video-level and frame-level—to facilitate efficient retrieval and flexible querying.

**Video-Level Metadata:** summarizes high-level annotations and semantic context:

- **Video ID:** Unique identifier for each video clip.
- **Person ID:** Unique identifier for annotated individuals within videos.
- **Action Labels:** Fine-grained human action labels.
- **Caption:** Detailed textual description of the video content.
- **Question-Answer Pairs:** Structured questions and answers related to video content.

**Frame-Level Metadata:** provides detailed annotations at individual frame granularity:

- **Video ID:** Corresponding identifier linking video-level metadata.
- **Frame stamp:** Temporal location of annotated frames within videos.
- **Person ID:** Unique identifier for each individual per frame.
- **Bounding Box:** Pixel coordinates (xmin, ymin, xmax, ymax) for each annotated person.
- **Clip Type:** Indicates real-world or cinematic origin of video clips.

Video naming follows the “[source identifier]\_[sequence number]” format, where the identifier is the YouTube ID or film name, and the sequence number indicates its temporal position. This structured metadata approach ensures efficient integration between frame-level and video-level annotations, effectively supporting downstream vision-language research in microgravity environments. For comprehensive documentation of the dataset metadata, please refer to the resources provided on our GitHub and Hugging Face repositories.

## F SUPPLEMENTARY FOR HUMAN ACTION RECOGNITION (HAR) TASK

### F.1 DATASET PARTITIONING

The dataset was partitioned at the video level following two primary criteria: (1) ensuring coverage of all action classes through greedy selection, and (2) proportional random splitting of remaining videos into training, validation, and test subsets (70:10:20 ratio). This approach avoids label leakage by maintaining video-level annotation consistency within subsets. Table 6 provides a summary of the sample-level and video-level distributions across splits.

Table 6: Train/val/test split statistics for the HAR task in MicroG-4M. Each cell reports both the absolute count and its corresponding percentage (%).

Split	Samples (# / %)	Video Clips (# / %)
Train	9,266 (69.93%)	3,331 (69.99%)
Val	1,329 (10.03%)	475 (9.98%)
Test	2,656 (20.04%)	953 (20.03%)
Total	13,251 (100.00%)	4,759 (100.00%)

### F.2 DATASET STATISTICS

Table 7 summarizes the distribution of three broad action types, namely Object Manipulation, Person Interaction, and Person Movement, across the entire dataset, cinematic subset, and real video subset. Object Manipulation constitutes the largest category, particularly within real videos (39.42%), followed by Person Interaction and Person Movement categories.

Table 8 presents statistics regarding the number of persons annotated per video. Single-person videos dominate the dataset, particularly in real footage (92.41%), while multi-person annotations are comparatively more frequent in cinematic sources.

Additionally, Table 9 provides a detailed breakdown of 50 fine-grained action classes. The most frequent actions across both subsets include ‘stand’, ‘carry/hold object’, and ‘talk to self/person’, whereas actions such as ‘climb’, ‘take photo’, and ‘kiss person’ are comparatively rare. Notably, the distribution of action labels exhibits a pronounced long-tail pattern, consistent with Zipf’s law commonly observed in naturally occurring datasets, indicating the realistic and representative nature of the collected action annotations.

Table 7: Label type distribution across the full dataset, cinematic subset, and real video subset. Each cell shows the number of labels followed by its proportion (%).

Label Type	All Videos	Movies	Real Videos
Object Manipulation	4,986 (37.60%)	1,416 (38.78%)	3,788 (39.42%)
Person Interaction	4,288 (32.34%)	1,198 (32.81%)	2,950 (30.70%)
Person Movement	3,987 (30.07%)	1,037 (28.40%)	2,872 (29.89%)

Table 8: Distribution of the number of persons per video in MicroG-4M. Each cell shows the number of videos followed by its proportion (%).

Persons per Video	All Videos	Movies	Real Videos
Single Person (1)	3,983 (83.69%)	816 (61.26%)	3,167 (92.41%)
Two Persons (2)	623 (13.09%)	395 (29.65%)	228 (6.65%)
Three or More ( $\geq 3$ )	153 (3.22%)	121 (9.09%)	28 (0.94%)

### F.3 PER-CLASS AP RESULTS

Figures 7 and 8 display the per-class average precision (AP) performance of models fine-tuned on MicroG-4M and AVA datasets, respectively, and evaluated on the MicroG-4M test set. Fine-tuning on MicroG-4M generally achieves higher per-class AP scores, highlighting improved model adaptation to microgravity-specific action patterns. In contrast, AVA fine-tuned models exhibit significant performance degradation, particularly on fine-grained or microgravity-specific actions such as ‘operate spaceship’, ‘float’, or posture-related actions (‘bend/bow’). These differences underscore the critical need for specialized fine-tuning datasets such as MicroG-4M to address the unique challenges posed by microgravity environments in action recognition tasks.

### F.4 CROSS-DATASET VQA DENSITY AND DESIGN RATIONALE

To contextualize our choice of six QA pairs per 3-second clip (**2 QA/s**), we compare MicroG-4M with representative video-VQA corpora in terms of clip granularity, QA density, and question types. This unified view allows controlled discussion of annotation budget and reasoning load across datasets with heterogeneous clip lengths.

MicroG-4M targets short clips at high QA density (2.00 QA/s), comparable to MSVD-QA and exceeding other widely used corpora. A fixed per-clip budget supports semantic diversity while avoiding redundancy typical of long-form settings. Our QA taxonomy balances *foreground actions*, *spatial context*, *entity/attribute grounding*, and *temporal/causal reasoning*, and explicitly includes an *unanswerable* option to reduce hallucination.

Because question generation protocols and scoring schemes vary across datasets, cross-corpus density should be interpreted as a *comparability aid* rather than a difficulty metric. The choice of six QA pairs per 3-second segment is thus motivated by controllability: it preserves clip-level coverage and evaluation stability while enabling *apples-to-apples* studies of domain shift in microgravity, independent of confounds from variable clip durations or QA volumes.

Table 9: Complete summary of action class distribution across all videos, movies, and real videos (sorted by action ID).

ID	Action Name	Count		
		All Videos	Movies	Real Videos
1	bend/bow (at waist)	26	14	12
3	crouch/kneel	20	2	18
5	fall down	10	1	9
6	get up	25	4	21
7	jump/leap	20	0	20
8	lie/sleep	17	4	13
9	martial art	18	0	18
10	run/jog	12	0	12
11	sit	252	239	13
12	stand	3218	698	2520
14	walk	369	75	294
17	carry/hold object	3126	549	2577
20	climb (e.g., mountain)	1	1	0
22	close (door/box)	13	4	9
24	cut	9	0	9
26	dress/undress clothing	31	9	22
27	drink	43	5	38
28	operate spaceship	20	16	4
29	eat	45	2	43
30	enter	68	5	63
34	hit object	33	3	30
36	lift/pick up	188	10	178
38	open (window/door)	32	13	19
41	play musical instrument	3	0	3
43	point to object	323	2	321
45	pull object	32	19	13
46	push object	24	8	16
47	put down	138	7	131
48	read	15	14	1
56	take photo	2	0	2
57	text/look at cellphone	7	0	7
58	throw	4	0	4
59	touch object	353	136	217
60	turn screwdriver	17	9	8
61	watch TV/unspecified	346	316	30
62	work on computer	110	67	43
63	write	3	3	0
64	fight/hit person	27	26	1
65	give/serve object	46	20	26
66	grab person	41	31	10
67	hand clap	3	3	0
68	hand shake	4	2	2
69	hand wave	140	44	96
70	hug person	16	13	3
72	kiss person	1	1	0
74	listen to person	148	135	13
76	push person	3	2	1
78	take object from person	15	10	5
79	talk to self/person	3131	504	2627
80	watch person	713	625	88

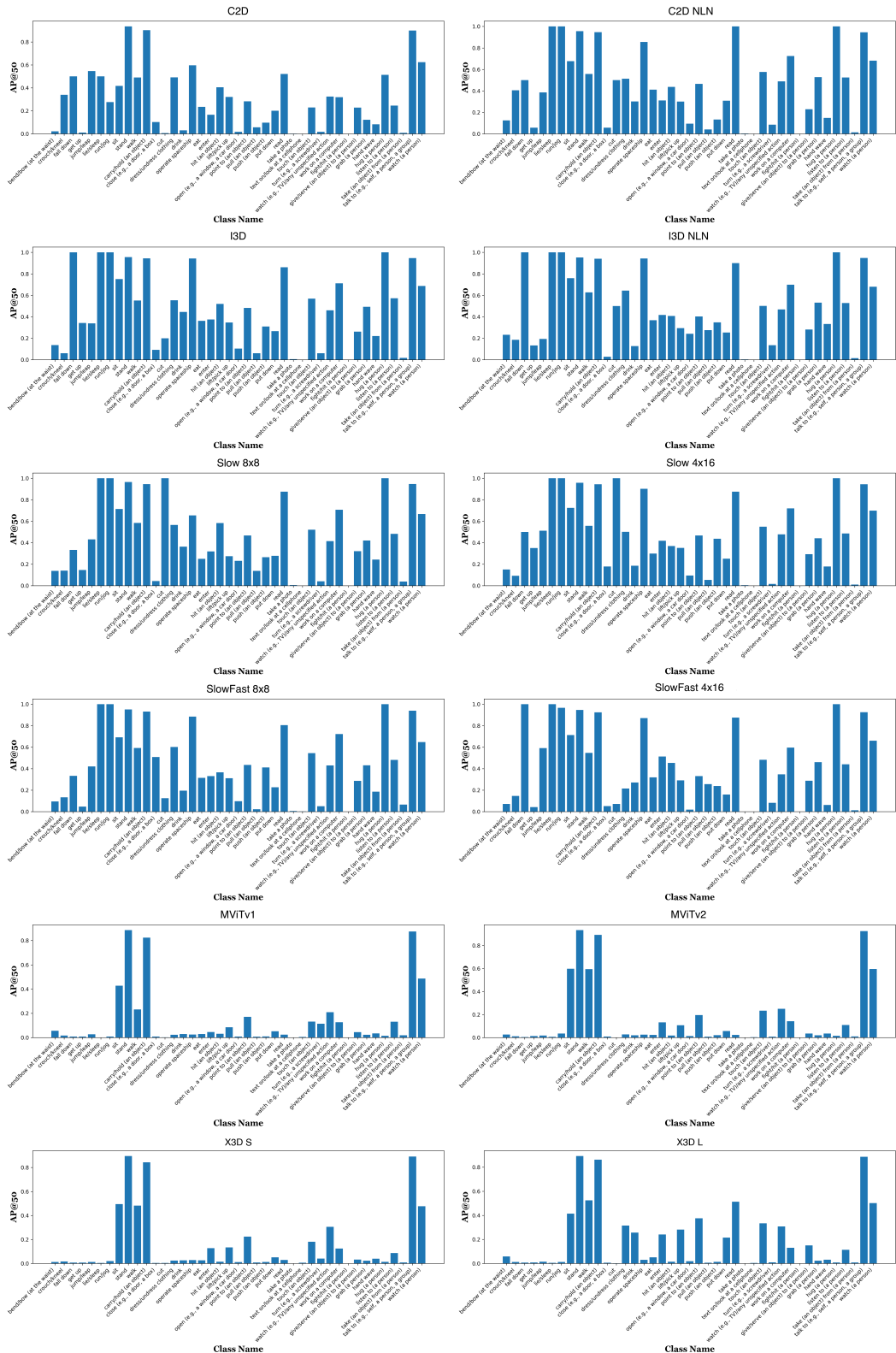


Figure 7: Per-Class AP after Fine-Tuning on MicroG-4M, evaluated on the MicroG-4M test set. All models shown in this figure correspond to those listed in Table 1 of the main text.

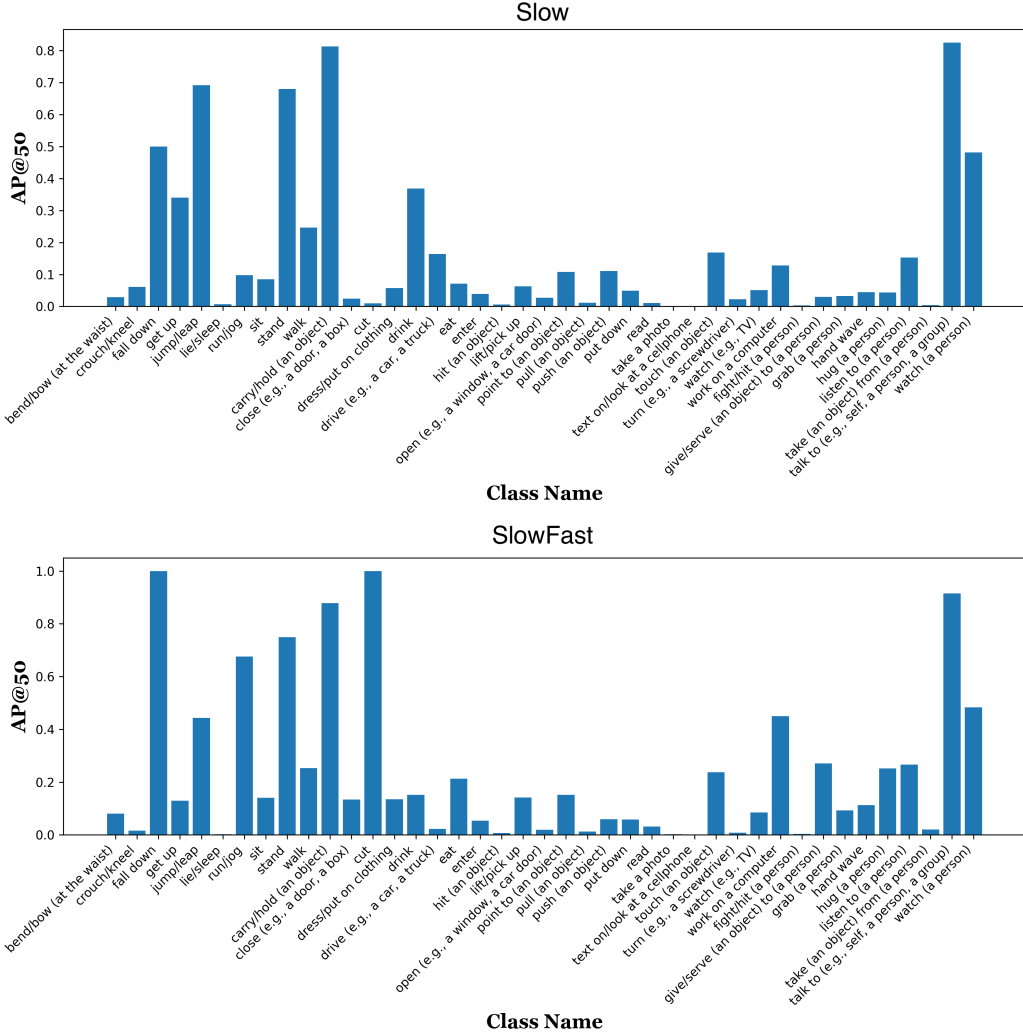


Figure 8: Per-Class AP after Fine-Tuning on AVA, evaluated on the MicroG-4M test set. All models shown in this figure correspond to those listed in Table 2 of the main text.

Table 10: Cross-dataset VQA density and scope. Statistics are compiled from the original dataset reports. “QA/sec” denotes (Avg. QA/Clip)/(Clip length in seconds). This comparison contextualizes our choice of six QA per 3-second clip in MicroG-4M.

Dataset	Clips	QA pairs	Avg. QA/Clip	Clip Len. (s)	QA/sec	QA Types
MSVD-QA Xu et al. (2017)	1,970	50,505	25.64	10	2.56	Wh-type
MSRVT-QA Xu et al. (2017)	10,000	243,680	24.37	15	1.62	Wh-type
TGIF-QA Jang et al. (2017)	56,720	103,919	1.83	3	0.61	Task-based
TVQA Lei et al. (2018)	21,793	152,545	7.00	76	0.09	Wh-type + Temporal
ActivityNet-QA Yu et al. (2019)	5,800	58,000	10.00	180	0.06	Motion, Spatial, Temporal
MovieQA Tapaswi et al. (2016)	6,771	6,462	0.95	200	0.004	Story comprehension
VideoQA Yang et al. (2003)	18,100	174,775	9.66	45	0.21	Wh-type + Yes/No
<b>MicroG-4M (Ours)</b>	<b>1,238</b>	<b>7,428</b>	<b>6.00</b>	<b>3</b>	<b>2.00</b>	<i>Wh-type, Foreground/Background, Fine-/Coarse-motion, Identity, Temporal, Causal</i>